

1 **Nitrogen redistribution and seasonal trait fluctuation facilitate plant N**
2 **conservation and ecosystem N retention**

3
4 Qingzhou Zhao^{1,2,8}, Peng Wang^{1,8}, Gabriel Reuben Smith², Lingyan Hu¹, Xupeng Liu¹,
5 Tingting Tao³, Miaojun Ma^{4,5}, Colin Averill², Grégoire T. Freschet⁶, Thomas Crowther²,
6 Shuijin Hu^{1,7,*}

7
8 ¹College of Resources and Environmental Sciences, Nanjing Agricultural University, Nanjing,
9 Jiangsu 210095, China

10 ²Department of Environmental Systems Science, ETH Zürich, Zurich 8092, Switzerland

11 ³Department of Earth and Environmental Sciences, The University of Manchester, Manchester
12 M13 9PL, United Kingdom

13 ⁴State Key Laboratory of Herbage Improvement and Grassland Agro-ecosystems, College of
14 Ecology, Lanzhou University, Lanzhou, Gansu 730000, China

15 ⁵Gansu Gannan Grassland Ecosystem National Observation and Research Station, Lanzhou
16 University, Gannan, Gansu 747312, China

17 ⁶Theoretical and Experimental Ecology Station, CNRS, Moulis 09200, France

18 ⁷Department of Entomology & Plant Pathology, North Carolina State University, Raleigh, NC
19 27695, United States

20 ⁸Qingzhou Zhao and Peng Wang should be considered co-first authors

21 * Author for correspondence: Shuijin Hu (shuijin_hu@hotmail.com)

22

23 **Summary**

- 24 1. Low available nitrogen (N) limits plant productivity in alpine regions and alpine plants thus
25 resorb and reallocate N from senescing tissues to conserve limiting N across the non-growing
26 season. However, the destination and the extent of N redistribution during plant senescence
27 among above- and belowground organs, let alone other processes of translocation outside of
28 the plants and into the soil components, remain poorly understood.
- 29 2. Utilizing ^{15}N stable isotope as a tracer, we quantified N redistribution among above- and
30 below-ground plant organs and different soil components during senescence in an alpine
31 meadow ecosystem, and explored the relationship between ^{15}N partitioning among plant-soil
32 N pools with seasonal fluctuations of plant functional traits.
- 33 3. We found substantial depletion of ^{15}N in fine roots ($-40\% \pm 2.8\%$) and aboveground tissues
34 ($-51\% \pm 5.1\%$), and important ^{15}N storage primarily in coarse roots ($+79\% \pm 27\%$) and soil
35 organic matter ($+37\% \pm 10\%$) during plant senescence. In parallel, we observed a temporal
36 variation in plant functional traits, representing a shift from more acquisitive to more
37 conservative strategies as the growing season ends, such as higher coarse root N and coarse
38 root: fine root ratio. Particularly, ^{15}N retention in particulate and mineral-associated organic
39 matter increased by $30\% \pm 12\%$ and $24\% \pm 9\%$, respectively, suggesting a potential pathway
40 through which fine root and microbial mortality contributes to ^{15}N redistribution into soil N
41 pools during senescence.
- 42 4. *Synthesis*. N redistribution and seasonal plant trait fluctuation facilitate plant N conservation
43 and ecosystem N retention in the alpine system. This study suggests a coupled aboveground-

44 belowground N conserving strategy that may optimize the temporal coupling between plant

45 N demand and ecosystem N supply in N-limited alpine ecosystems.

46

47 **Keywords:** functional traits, N resorption, N retention, ¹⁵N labeling, plant nutrient strategies,

48 plant-soil interactions, soil organic matter

49

50 **1. Introduction**

51 Nutrient limitation is a major constraint of terrestrial plant performance and primary
52 productivity worldwide (Lambers, Chapin III & Pons 2008; Du *et al.* 2020). Nutrient
53 conservation thus plays a crucial role in plant adaptation to infertile environments, especially in
54 extremely nitrogen (N)-limited alpine regions (Parton *et al.* 2007; Fisher *et al.* 2010; Freschet
55 *et al.* 2010). Plants have multiple strategies to conserve limiting nutrients, such as extending
56 the lifespan of plant tissue or retranslocating nutrients from senescing tissues to limit losses
57 (Chapin III & Kedrowski 1983; Eckstein, Karlsson & Weih 1999). In particular, perennial
58 plants withdraw up to ~60% of N from their senescing tissues, accounting for over 31% of their
59 total annual N demand (Vergutz *et al.* 2012; Deng *et al.* 2018). This N retranslocation from
60 senescing leaves (i.e., N resorption) significantly affects plant regrowth (Lü *et al.* 2019),
61 community composition (Lü *et al.* 2021), and ecological succession (Hayes *et al.* 2014).
62 However, the fate of N resorbed from senescing plant organs and its relationship with the plant
63 functional traits remains poorly understood, whether at the level of shoot-root N budget or for
64 ecosystem N cycling (Freschet *et al.* 2010; Daly *et al.* 2021).

65 Most studies exploring N resorption from above- or below-ground plant components have
66 focused on responses that occur at the organ level and often neglected shoot-root and plant-soil
67 interactions that occur at the community level. While N resorption can mediate plant species
68 co-existence, vegetation regrowth and succession over time at the community level (Hayes *et al.*
69 *et al.* 2014; Lü *et al.* 2019), it influences litter chemistry and ecosystem N retention and cycling
70 at the ecosystem level (Deng *et al.* 2018; Wang *et al.* 2018). Nutrient conservation is an
71 important aspect of plant adaptation, community succession, vegetation distribution, and

72 ecosystem N retention across different spatial and temporal scales. However, our understanding
73 of these processes is limited by the lack of knowledge on seasonal N fluxes involving
74 belowground organs at the community and ecosystem levels. Yet, roots and other belowground
75 organs can comprise over 85% of the total plant biomass in some alpine grasslands (Yang *et al.*
76 2009; Ma *et al.* 2021), and fine-root production accounts for 22% of global terrestrial net
77 primary production (McCormack *et al.* 2015). The extent to which fine-root N is resorbed
78 during senescence largely remains unclear. While some local-scale studies showed little change
79 in fine-root N concentration during senescence (Nambiar 1987; Aerts 1990; Gordon & Jackson
80 2000), others reported substantial N resorption in both woody and non-woody perennials
81 (Woodmansee, Vallis & Mott 1981; Meier, Grier & Cole 1985; Freschet *et al.* 2010). This
82 discrepancy may stem from different definitions of fine roots (McCormack *et al.* 2015), the
83 sampling of non-natural phenological root senescence (Aerts, Bakker & De Caluwe 1992), or
84 from different estimation methods (Kunkle, Walters & Kobe 2009). Recently, Kunkle *et al.*
85 (2009) re-analyzed published results by correcting root mass loss and found an N decrease of
86 28% in recently senescing fine roots, suggesting an underestimation of N retranslocation from
87 fine roots. On the other hand, roots and rhizomes of many deciduous woody species and
88 herbaceous plants play an essential role in nutrient storage during winter (Millard & Grelet
89 2010; Zadworny *et al.* 2015; Cong *et al.* 2019; Zhao *et al.* 2020), indicating their dual role as
90 N sink and source during senescence (Gordon & Jackson 2000).

91 A growing body of evidence highlights how trait-based approach can be useful for
92 understanding the trade-offs governing plant physiological responses to environmental change.
93 Spatial and temporal changes in climatic and soil conditions have well-known effects on plant

94 nutrient strategies (Reich 2014; Vitra *et al.* 2019; Joswig *et al.* 2021; Keep *et al.* 2021). In turn,
95 changes in plant functional traits interact with seasonal and longer temporal changes in
96 environmental stresses to affect essential ecosystem processes (Chapin III & Kedrowski 1983;
97 Lambers *et al.* 2008). For example, plants with lower N resorption can allocate more nutrient
98 belowground responding to seasonal drought and species with stronger resorption enhanced
99 aboveground investment under N enrichment (Zhao *et al.* 2020). In environments with low
100 temperature and nutrient availability, leaf N content, specific leaf area, fine-root N content and
101 specific root length decrease at the end of the growing season (Zadworny *et al.* 2015; Vitra *et*
102 *al.* 2019), but biomass and N content in transportive roots likely increase (Zadworny *et al.* 2015;
103 Cong *et al.* 2019). However, the seasonal trait variations and their linkage with N conservation
104 in natural ecosystems have not been extensively studied (Freschet *et al.* 2010). Understanding
105 to what extent the process of nutrient redistribution, both above- and below-ground, is
106 paralleled with temporal shifts in acquisitive versus conservative trait expression in plants will
107 help us refine our knowledge of plant nutrient strategies and ecosystem N dynamics.

108 At the ecosystem level, N is a major constituent of living plants, litter, soil microbial
109 biomass and soil organic matter (SOM). Differential partitioning among these N pools can
110 critically affect cumulative N retention with consequences on the cycling of other elements,
111 such as ecosystem C accumulation (Hu *et al.* 2001; Jia *et al.* 2022). For example, N in senescing
112 tissues can be redistributed into plant biomass, or transferred to SOM through rhizodeposition
113 and litterfall (Aerts, Verhoeven & Whigham 1999; Kunkle, Walters & Kobe 2009; Bernard *et*
114 *al.* 2022). Particularly, mineral N can be incorporated into and released from two generally
115 classified SOM pools, particulate organic matter (POM) and mineral-associated organic matter

116 (MAOM), and these forms of N have different availability for plants according to different
117 growing seasons (Sollins, Homann & Caldwell 1996; Schimel & Bennett 2004; Jilling *et al.*
118 2018). During the growing season, the availability of N from POM and MAOM for plants
119 differs because several factors such as microbial activity, temperature and moisture influence
120 N mineralization rates (Shahzad *et al.* 2012; Bernard *et al.* 2022). For instance, during the peak
121 growing season, high microbial activity and high temperature can lead to high N mineralization
122 of POM. In comparison, N in MAOM is more protected by soil matrix and is less available for
123 plants. Low temperature and microbial activities often constrain N mineralization and N
124 availability for plants. Depending on plant nutrient demand at different growing stages, SOM
125 may serve as a nutrient reservoir or supplier (Lambers *et al.* 2008; Chapin III, Matson &
126 Vitousek 2011). However, we need a more holistic approach to examine N fluxes within the
127 plant-soil-microbe system to understand their direct consequences for plant N conservation and
128 indirect implications for ecosystem N retention and C sequestration, especially for N-limited
129 alpine regions.

130 Here, we investigated the N redistribution among most N pools in a Tibetan alpine meadow
131 with high N limitation. Specifically, we used ¹⁵N stable isotope to track seasonal N
132 redistribution among plant organs and soil fractions and to explore the linkage between plant-
133 soil N fluxes and plant functional traits during plant senescence. We hypothesized that 1) at the
134 plant community scale, alpine plants will withdraw N from aboveground tissues and fine roots
135 but enhance the N storage in rhizomes and coarse roots during senescence, 2) plant senescence
136 and its associated N redistribution correlate with a shift in functional traits towards more
137 resource-conservative strategies upon the end of the growing season, and 3) N fluxes from

138 plants and microbes to soil during plant senescence constitute a significant pathway of N
139 retention in soil organic matter. We tested these hypotheses using mesocosms in the field and
140 ^{15}N tracing *in situ* by quantifying the redistribution of ^{15}N among different N pools between
141 vegetation growth peak and the end of the growing season.

142

143 **2. Materials and Methods**

144 **2.1 Study site and experimental design**

145 Our study site is located at the Qinghai-Tibetan Plateau, the highest and largest plateau on the
146 Earth, and local ecosystems are highly N-limited (Du *et al.* 2020). Over 50% of its area is
147 covered by natural alpine grasslands (Ni 2000), with little human disturbance, providing an
148 ideal place to study seasonal N redistribution. This study was based at the Gansu Gannan
149 Grassland Ecosystem National Observation and Research Station (33°68' N, 101°88' E; 3538
150 m a.s.l.) in the eastern Tibetan Plateau, Maqu County, Gansu Province, China. The climate of
151 the ecoregion is a cold-humid alpine climate, with a mean annual temperature of 1.2 °C and
152 mean annual precipitation of 590 mm over the last 50 years, and the precipitation mainly occurs
153 during the short-cool summer (Xu *et al.* 2021). The growing season spans from early May to
154 October. The soil type is Cambisol in FAO/UNESCO taxonomy, with a pH at 6.0, soil total C
155 at 98.2 g C kg⁻¹, and soil total N at 6.9 g N kg⁻¹ soil in the top 10 cm (Zhang *et al.* 2020). The
156 vegetation type is an alpine meadow mainly dominated by perennial sedges (e.g., *Kobresia*
157 *capillifolia*, *Kobresia tibetica*, *Carex moorcroftii*), grasses (e.g., *Elymus nutans*, *Stipa aliena*,
158 *Festuca ovina*), compositae species (e.g., *Aster diplostephioides*, *Ligularia virgaurea*), and
159 other forb species (e.g., *Polygonum viviparum*, *Gentiana algida*) (Wang *et al.* 2020). Based on

160 the species survey in this study, non-perennial herbs are rare, accounting for about 2% and 6%,
161 and perennial plants account for about 98% and 94% of the aboveground biomass and
162 abundance, respectively.

163 We established the experiment in an undisturbed area on a gentle southeastern-facing slope
164 by setting up six pairs of mesocosms with similar plant compositions. In the early growing
165 season (May 23rd) of 2021, six pairs of PVC pipes (inner diameter: 19 cm, height: 22 cm) were
166 hammered into the soil to 20 cm deep as semi-closed systems. The top of the PVC pipes was 2
167 cm above the ground to prevent any horizontal water movement between the PVC tubes and
168 the adjacent areas. Each pair of PVC pipes were 2 - 10 cm away from each other, and the
169 distance between pairs was 2 - 5 m. On July 2nd, 2021, after six weeks of plant growth and soil
170 stabilization, plant litter on the soil surface and standing dead stalks were removed. Then,
171 16.931 mg ^{15}N in a 120 ml solution (5 ppm, 75.698 mg $(^{15}\text{NH}_4)_2\text{SO}_4$, 98% atom ^{15}N) was
172 evenly injected through 24 locations at two soil depths (2 cm and 5 cm) within each pipe. Light
173 rain in the subsequent days following the ^{15}N injection facilitated the homogeneity of the ^{15}N
174 labeling. Four unlabeled parallel mesocosms (PVC pipes) were established in the same
175 undisturbed area following the same experimental steps as other mesocosms described above,
176 to determine the natural ^{15}N abundance of plant and soil components at the growth peak period.

177

178 **2.2 Plant-soil sampling and measurements**

179 On August 13th, 2021, six weeks after ^{15}N injection, when vegetation in this region reaches a
180 peak primary productivity with their highest N assimilation, one mesocosm of each pair was
181 harvested by pulling the PVC pipes out, together with the plants and soil. The subsoil (20 - 25

182 cm depth, ca. 100g) was also collected below each pipe. Aboveground plant communities were
183 cut at the soil surface, separated by species, oven-dried (48 °C, 48 hrs), and weighed as shoot
184 biomass. The total weight of the soil in each pipe was recorded, and then manually sorted into
185 roots and soils and sieved through a 2 mm sieve. Following this procedure, soil samples were
186 timely stored at 4°C (500 g) and -20 °C (100g) before laboratory analyses. Roots were
187 thoroughly washed, air-dried for 12 hours indoors (temperature: 10 °C; air humidity: 50 - 70%),
188 and then weighed as the fresh root mass. A representative subsample of fresh roots (10 g) was
189 manually separated into fine roots (FR, absorptive roots, root order 1 - 2) and coarse roots (CR,
190 transportive roots and rhizomes, root order ≥ 3) for morphological analyses. Another subsample
191 of fresh roots of 5 g was left un-separated for morphological analyses of entire-root traits. The
192 remaining root samples were oven dried (48 °C, 48 hrs) and weighed. For the second mesocosm
193 in each pair, the fresh leaf litter was timely collected twice, on August 13th and August 28th,
194 2021, to limit material loss via leaching and decomposition. At the end of the growing season
195 on October 10th, 2021, senescent plants (including leaves that remain green at the start of
196 winter), soil cores and subsoils of the second mesocosm of each pair were sampled and
197 processed as described above for the peak biomass stage (the first mesocosm of each pair).

198 To examine whether paired plant community composition and species biomass differed
199 across the growing stages, we compared diversity indices of paired community composition
200 and the principal coordinates analysis (PCoA) of the overall differences between species
201 biomass structure (Figs S1–S2). We observed no significant difference and thus concluded that
202 our temporal approach based on paired sampling was appropriate for linking aboveground and
203 belowground N relocation during plant senescence.

204

205 **2.3 Determination of plant, soil, and microbial properties**

206 Soil moisture, pH, ammonium (NH_4^+) and nitrate (NO_3^-), available phosphorus (AP), soil
207 dissolved organic C (DOC) and N (DON), K_2SO_4 extractable N (EN), and microbial biomass
208 C (MBC) and N (MBN) were measured as described by Xu *et al.* (2021)) for the same study
209 site. Soils were fractionated by two particle size classes: particulate organic matter (POM, > 53
210 μm) and mineral-associated organic matter (MAOM, $\leq 53 \mu\text{m}$) using a wet sieving approach
211 (Yan, Wang & Yang 2007). Fresh samples of coarse roots and fine roots were scanned with
212 backlighting (Epson Expression 12000XL-PH, Japan), and images were processed with
213 WinRHIZO 2020a (Regent Instruments Inc., Canada) to determine root morphological
214 parameters (root diameter, length, surface area, and volume were recalculated as the sum of the
215 values provided for each diameter classes, as values provided by WinRHIZO 2020a are
216 inaccurate). Specific root length (SRL) and specific root area (SRA) were estimated by dividing
217 root length and surface area by the dry weight, respectively. Root tissue density (RTD) was
218 calculated by dividing root dry mass by fresh root volume. For coarse roots, we eliminated the
219 length, surface area, and volume of the remaining truncated base of separated fine roots,
220 identified as the following root diameter class: $0 < \text{Diameter-Class} < 0.5 \text{ mm}$, because it can
221 lead to severely inaccurate estimation of coarse root diameter, specific root length (SRL), and
222 specific root area (SRA), especially for grasses (Freschet *et al.* 2021a). Root mass fraction was
223 calculated by dividing root biomass by entire plant biomass. Oven-dried plant shoots (total
224 aboveground biomass including leaves that remain green and pre-collected fresh leaf litter for
225 the senescent stage), coarse roots, fine roots, soils, POM and MAOM were separately ground

226 into fine powder with a ball mill (Retsch MM200, Germany). C and N concentrations were
227 determined by an elemental analyzer (Vario MICRO cube, Elementar, Germany), and ^{15}N
228 atomic percentage (AT% [^{15}N]) was determined by EA-IRMS (DELTA V Advantage, Thermo
229 Fisher Scientific, USA).

230

231 **2.4 Estimation of ^{15}N partitioning and redistribution efficiencies in shoot, root, soil, and** 232 **their sub-fractions**

233 We quantified ^{15}N partitioning (as measured by ^{15}N recovery rate, i.e. ^{15}NRR) at two plant
234 growing stages among eight N pools (plant shoot, fine roots, coarse roots, soil, POM, MAOM,
235 K_2SO_4 -extractable dissolved N and microbial biomass N), and estimated the percentage change
236 in ^{15}N recovery (denoting ^{15}N redistribution efficiency) in each N pool. AT% [^{15}N] and N
237 concentration in ^{15}N labeled shoots, coarse roots, fine roots, and soil fractions were determined
238 on EA-IRMS as described above. Microbial biomass AT% [^{15}N] was determined after Kjeldahl
239 digestion and diffusion (Stark & Hart 1996). Non-extractable ^{15}N content (NEOM pool, mostly
240 organic ^{15}N) was calculated by subtracting microbial biomass ^{15}N and K_2SO_4 -extractable ^{15}N
241 (EN pool) from total soil ^{15}N . The field plots were fenced to prevent disturbance from large
242 herbivores. Additionally, the proportion of gaseous nitrogen loss is quite low within such a
243 brief experimental period (Zhang *et al.* 2020). The ^{15}N detected in the subsoil of the mesocosms
244 accounted for only 1.6% of the total (Fig. 1), leading us to infer that N leaching was minimal
245 during the experimental period. Consequently, we attributed all potential ^{15}N losses to the
246 unrecovered ^{15}N pool.

247 The percentage of ^{15}N recovery in all N pools was calculated as N concentration multiplied
 248 by the biomass or mass of each pool, then multiplied by the difference of AT% [^{15}N] between
 249 labeled and natural samples, and finally divided by ^{15}N tracer applied. So, the ^{15}N recovery
 250 rates in each plant and soil fractions were calculated following Equation 1:

251

$$252 \quad {}^{15}\text{NRR} = \frac{[\text{N}] \times \text{mass} \times (\text{AT}\% [^{15}\text{N}]_{\text{labeled}} - \text{AT}\% [^{15}\text{N}]_{\text{natural}})}{{}^{15}\text{N}_{\text{added}} \times (\text{AT}\% [^{15}\text{N}]_{\text{tracer}} - \text{AT}\% [^{15}\text{N}]_{\text{natural}})} \times 100\% \quad (\text{Eqn 1})$$

253

254 Where $\text{AT}\% [^{15}\text{N}]_{\text{tracer}}$, $\text{AT}\% [^{15}\text{N}]_{\text{labeled}}$, $\text{AT}\% [^{15}\text{N}]_{\text{natural}}$ represent the atomic percentage value
 255 ($^{15}\text{N}/(^{15}\text{N} + ^{14}\text{N})$) of the tracer, labeled, and background samples, respectively; [N], mass, and
 256 $^{15}\text{N}_{\text{added}}$ represent N concentration in each N pool, biomass/mass of each pool at the time of
 257 sampling, and mass of ^{15}N tracer applied, respectively.

258 Although changes in plant N concentrations have been typically used to calculate N
 259 resorption efficiency, they are inadequate as a quantitative metric of N redistribution among
 260 shoot-root tissues because organ biomass may also change during senescence (van
 261 Heerwaarden, Toet & Aerts 2003; Kunkle, Walters & Kobe 2009). We therefore examined N
 262 pools instead of N concentration to evaluate ^{15}N redistribution in each N pool. The ^{15}N
 263 redistribution efficiency in each N pool was calculated as the percentage change in ^{15}N recovery
 264 rate between growth peak period and the end of the growing season following Equation 2:

265

$$266 \quad \% \text{ change in } ^{15}\text{N recovery} = \frac{{}^{15}\text{NRR}_{\text{senescence stage}} - {}^{15}\text{NRR}_{\text{growth peak}}}{{}^{15}\text{NRR}_{\text{growth peak}}} \times 100\% \quad (\text{Eqn 2})$$

267

268 Here, $^{15}\text{NRR}_{\text{growth peak}}$ and $^{15}\text{NRR}_{\text{senescence stage}}$ represent the ^{15}N recovery rate in a given
269 ecosystem N pool at the vegetation growth peak and the end of the growing season, respectively.
270 For each plant or soil component, a positive value of % change in ^{15}N recovery indicates ^{15}N
271 storage pools, while negative values denote ^{15}N depletion pools during plant senescence.

272

273 **2.5 Statistical analysis**

274 All statistical analyses were conducted using R (version 4.0.2) (R 2021). Student's paired t-
275 tests were used for comparisons of soil properties, microbial properties, ^{15}N distribution and
276 nutrient allocation between the two growing season stages. To investigate the temporal
277 transition of plant economics spectrum, we conducted a principal component analysis (PCA)
278 including sixteen root traits and two shoot traits at the community level with 95% prediction
279 ellipses. Pearson's correlations were performed to examine the relationships of ^{15}N recovery
280 among different plant and soil components with changes across plant growth stages, in terms
281 of soil and microbial properties, plant nutrient concentrations and biomass allocation, and root
282 morphology. Diversity indices of plant communities (Shannon-Wiener index, Simpson index,
283 species richness, and species evenness) were calculated to examine any potential differences
284 in community structure between the two plant growth stages across each pair of mesocosms
285 using a student's paired t-test. In addition, a principal coordinate analysis (PCoA) was
286 performed to analyze the differences in community structure (aboveground-biomass-based)
287 between two growth stages based on Bray-Curtis distances under Robust Scaler standardization.
288 We set the significance level at $P < 0.05$.

289

290 **3. Results**

291 **3.1 Soil and microbial properties across the growing season**

292 From August 13th to October 10th, inorganic soil N and soil available phosphorus decreased
293 (Table 1, $P < 0.01$). Similarly, DOC, DON, MBC and MBN decreased, with microbial biomass
294 being positively correlated with DOC and DON ($P < 0.05$). Soil pH increased by 0.14 units (P
295 < 0.05). Soil moisture, soil C:N ratio, and C and N concentrations in POM and MAOM showed
296 no significant change between the two sampling dates (Table 1).

297

298 **3.2 ^{15}N redistribution among different N pools**

299 The partitioning of total ^{15}N as measured by the percentage of ^{15}N recovery from different N
300 pools in the whole root system did not differ between the peak ($14.9\% \pm 0.97\%$, mean \pm SE,
301 the same below) and the end ($14.8\% \pm 0.97\%$) of the growing season (Fig. 1, $P = 0.94$). This
302 resulted in a neutral ^{15}N redistribution at the scale of whole-root system (% change in ^{15}N
303 recovery = $2.4\% \pm 11.5\%$, Fig. 2a). However, ^{15}N recovery in coarse roots increased from 5.38%
304 $\pm 0.36\%$ (mean \pm SE, the same below) at the peak biomass stage to $9.11\% \pm 1.36\%$ at plant-
305 senesced stage ($P = 0.026$). Conversely, ^{15}N recovery in fine roots declined from $9.55\% \pm 1.00\%$
306 at the peak biomass stage to $5.71\% \pm 0.57\%$ at the senescence stage ($P = 0.001$, Fig. 1), leading
307 to a negative % change of ^{15}N in fine roots during plant senescence ($-39.9\% \pm 2.81\%$, Fig. 2a).
308 For aboveground plant tissues (including leaves, stems, flowers, seeds, and fresh litter), the ^{15}N
309 recovery substantially decreased by half from $25.5\% \pm 1.32\%$ to $12.3\% \pm 0.95\%$ after plant
310 senescence ($P = 0.001$, Fig. 1), corresponding to a negative % change of ^{15}N in aboveground
311 tissues ($-50.94\% \pm 5.13\%$, Fig. 2a).

312 ^{15}N recovery in bulk soil increased from $30.1\% \pm 0.92\%$ to $36.5\% \pm 1.86\%$ from August
313 13 to October 10 ($P = 0.027$), with increases from 15.4% to 19.6% ($P = 0.038$) in POM and
314 from 12.7% to 15.5% ($P = 0.027$) in MAOM (Fig. 1), corresponding to a positive % change
315 of ^{15}N as $29.80\% \pm 11.84\%$ in POM and $24.30\% \pm 9.16\%$ in MAOM (Fig. 2b). Besides, ^{15}N
316 recovery in MBN and K_2SO_4 -extractable N pool (EN) significantly decreased from 5.77% to
317 4.64% ($P = 0.04$), and from 1.07% to 0.25% ($P < 0.001$), respectively (Fig. 1). As a result,
318 $76.58\% \pm 2.92\%$ and $17.85\% \pm 6.20\%$ of ^{15}N from EN and MBN, respectively, moved into
319 other pools (Fig. 2b). On the contrary, ^{15}N recovery in non-extractable soil organic matter
320 (NEOM) increased from 23.3% to 31.6% at the end of the growing season ($P < 0.05$, Fig. 1),
321 corresponding to a % change of ^{15}N as $37.4\% \pm 10.4\%$ in NEOM (Fig. 2b). Due to potential
322 ^{15}N loss pathways, such as gaseous N losses, herbivores consumption, seed dispersal and some
323 litter loss, there was more (6.9%) unrecovered ^{15}N with time (Fig. 1).

324

325 **3.3 Above- and below-ground plant economics traits at different growing stages**

326 A principal component analysis (PCA) suggested a temporal shift of the plant community along
327 the plant economics spectrum, moving from a more acquisitive strategy to a more conservative
328 strategy during senescence (Fig. 3). The first PCA axis accounted for 54.6% of the variance,
329 mainly defined by coarse root (CR)-N (element concentration, the same below), CR-C:N, CR
330 mass fraction, CR:FR ratio, FR-SRL, FR-SRA, FR-C, FR-N, FR-C:N, Shoot-N and Shoot C:N
331 (all traits significantly changed during senescence, Figs 4–5); and the second PCA axis was
332 mainly driven by coarse root morphological traits (i.e., CR-RTD, CR-SRL and CR-RD, Fig. 3).
333 We defined the first PCA axis as a conservation axis according to the representative plant traits.

334 Specifically, the root: shoot ratio ($P = 0.046$), coarse root mass fraction (CRMF, $P = 0.019$),
335 and coarse-root: fine-root ratio (CR:FR, $P = 0.038$) increased at the end of the growing season
336 (Fig. S3). Substantial N resorption occurred in shoots and fine roots, as their N concentration
337 decreased at the end of the growing season ($P = 0.01$, $P = 0.007$, respectively, Fig. S3). In
338 addition, C concentration in all belowground organs and fine roots significantly increased ($P =$
339 0.002 , $P = 0.017$, respectively), corresponding to declines of shoot C:N ratio and FR C:N ratio
340 ($P = 0.034$, $P = 0.003$, respectively, Fig. S3). Meanwhile, N concentration in CR significantly
341 increased during plant senescence ($P = 0.036$), matching the reduction of the CR C:N ratio (P
342 $= 0.038$, Fig. S3). According to root morphology, the FR-SRL and FR-SRA decreased by 29%
343 ($P = 0.018$) and 19% ($P = 0.013$), respectively, and fine-root diameter (FR-RD) increased from
344 0.20 to 0.23 mm during plant senescence ($P = 0.06$, Fig. S4). In other words, fine roots became
345 thicker and shorter during plant senescence.

346

347 **3.4 Correlations of ^{15}N partitioning to plant traits and edaphic properties**

348 ^{15}N recovery in whole-plant, shoots, and extractable soil N showed positive correlations with
349 available soil nutrients, DON, MBN, and bulk soil total N at both growing stages ($P < 0.05$,
350 Fig. S5b). ^{15}N recovery in FR, EN and MBN pools showed similar positive relationships with
351 soil NO_3^- , DON, and MBN ($P < 0.05$, Fig. S5b). Furthermore, ^{15}N recovery in MAOM showed
352 positive relationships with C and N concentrations of MAOM, but negative relationships with
353 that of POM ($P < 0.05$, Fig. S5b). Moreover, ^{15}N recovery in FR, EN and MBN pools were
354 positively related to graminoid biomass, shoot N, FR N and CR C:N ratio ($P < 0.05$) but
355 negatively related to CR:FR ratio, root C, FR C, CR N, shoot and FR C:N ratio ($P < 0.05$, Fig.

356 S5a). Interestingly, ^{15}N recovery in fine roots and coarse roots showed contrary relationships
357 with variables representing acquisitive-conservative strategies for nutrient allocation trade-off
358 (Fig. S5a). Specifically, ^{15}N recovery in fine roots was positively related to acquisitive-
359 allocation traits, including graminoid biomass, shoot-N, FR-N, CR-C:N, SRL, SRA, FR-SRL,
360 FR-SRA ($P < 0.05$; Fig. S5). In contrast, ^{15}N recovery in coarse roots was positively correlated
361 with conservative-allocation traits, such as root-C, FR-C, CR-N, shoot-C:N, FR-C:N, RD, FR-
362 RTD ($P < 0.05$; Fig. S5). Besides, ^{15}N recovery in coarse roots was positively related to entire-
363 root diameter and FR-RTD but negatively related to FR-SRL and FR-SRA (Fig. S5c), with
364 which fine-root ^{15}N recovery showed positive correlations. ^{15}N recovery in whole plants, shoots,
365 and fine roots showed similar correlations with plant nutrient traits, including shoot-N, FR-N,
366 CR-C:N ratio (positive correlations), and root-C, shoot-C:N ratio (negative correlations, Fig.
367 S5a). Besides, ^{15}N recovery in bulk soil, as well as in POM and NEOM, was positively
368 correlated with CR:FR ratio, root C, FR-C, and CR-N ($P < 0.05$, Fig. S5a), and negatively
369 correlated with DON, NO_3^- , MBC and MBN across growing stages ($P < 0.05$, Fig. S5b).

370

371 **4. Discussion**

372 Nitrogen conservation during plant senescence benefits plant fitness and vegetation regrowth.
373 Seasonal trait fluctuation from acquisitive to conservative may help plants to maximize nutrient
374 use efficiency as plants move from peak growth to senescence. Yet, our knowledge of root traits
375 and their relationship with N conservation lags far behind our understanding of aboveground
376 parts. Through tracing ^{15}N movement, our study provided direct evidence illustrating that
377 during the senescence process, coarse roots served as the major N storage due to increases in

378 both coarse root mass and N concentration, whereas fine roots and shoots showed major N
379 resorption. More interestingly, seasonal changes in ^{15}N recovery among plant organs covaried
380 with a temporal shift of traits, which defining the plant nutrient strategies of the grassland
381 community, from fast acquisition at the peak of plant growth to strong conservation at the end
382 of plant senescence.

383

384 **4.1 Roots play a dual role as both sink and source in N conservation**

385 We observed a substantial depletion of ^{15}N in fine roots and aboveground tissues, and a
386 increased ^{15}N storage primarily in coarse roots and soil organic matter during plant senescence
387 (Figs 1–2 and 7). The extent of N redistribution in total aboveground plant tissues ($-50.9\% \pm$
388 5.13%) based on changes in N pools is in line with previous estimates from N concentration in
389 herbaceous species (Aerts 1996; Yuan & Chen 2009), but lower than global estimates of 62.1%
390 after leaf mass loss correction (Vergutz *et al.* 2012). Although previous studies based on N
391 concentration did not observe significant N redistribution in senescing fine roots (Nambiar
392 1987; Aerts 1990; Gordon & Jackson 2000), our ^{15}N -pool-based approach allowed us to
393 observe substantial fine-root N redistribution ($39.9\% \pm 2.8\%$), which is higher than a global
394 estimation of 28% (Kunkle, Walters & Kobe 2009). Yet, the extent of N redistribution from
395 fine roots into other N pools may still be underestimated due to the potential mismatch between
396 root sampling and complete root senescence. Further, in contrast to leaves, not all fine roots are
397 meant to senesce at the end of the growing season (i.e. a mixture of living and senescing fine
398 roots), suggesting that at the level of one actively senescing root resorption might be much
399 stronger than recorded over the entire fine root pool. Finally, the ^{15}N tracing method cannot

400 fully recover all the ^{15}N applied, owing to gaseous N losses, herbivores consumption, seed
401 dispersal, and some litter loss. These potential ^{15}N loss pathways could explain the increase in
402 the unrecovered ^{15}N pool. On the other hand, some ^{15}N in newly produced root litter may have
403 been decomposed, mineralized and even re-acquired by roots. This means changes in root ^{15}N
404 recovery are not solely due to N retranslocation during senescence. Considering this caveat,
405 the ^{15}N retranslocation in fine roots can be overestimated slightly. Importantly, we observed a
406 significant increase in the coarse root ^{15}N pool during plant senescence ($+79.0\% \pm 27.1\%$),
407 supporting our first hypothesis that coarse roots and/or rhizomes act as major N storage tissues
408 during plant senescence. In other words, roots may play a dual role in herbaceous plant N
409 conservation across the year, with coarse roots acting as an N storage and fine roots as a N
410 recycling source (Gordon & Jackson 2000; De Vries *et al.* 2012; Freschet *et al.* 2021b). Our
411 results indicate that the overall change in root N pool alone during plant senescence likely fails
412 to tell the complete story of plant internal N translocation, especially among fine and coarse
413 roots.

414

415 **4.2 Linking seasonal plant economics traits with ^{15}N partitioning in plant-soil components**

416 In line with our second hypothesis, plant N redistribution during plant senescence went along
417 with a temporal shift in plant nutrient strategies from acquisitive to conservative (Fig. 4). At
418 the peak of their growth, plants are characterized by a more acquisitive strategy to meet higher
419 plant C and N demand, resulting in higher N partitioning to N-acquisitive plant organs (shoot
420 and fine roots), also as evidenced by strong correlations between N partitioning in N-acquiring
421 fractions and acquisitive plant traits (Shoot-N; FR-N; SRL; SRA) in our study (Fig. 4).

422 Nevertheless, Freschet *et al.* (2010) found relative independence of plant N and P resorption
423 from other economics traits and suggested that the dependence of nutrient resorption processes
424 on plant water uptake capacity and resistance to early frosts could partly explain this lack of
425 relationship. Previous works analyzing the relationships between plant economics strategy and
426 the ability of plants to re-translocate nutrients during senescence have based their comparisons
427 on plant functional traits, typically measured at the peak of plant growth (Weigelt *et al.* 2021).
428 Taking a perspective from the senescence progression, plants tended to conserve more nutrients
429 to survive for potential growth, leading to higher N retention in N-reserving organs (De Vries
430 *et al.* 2012; Wang *et al.* 2018). Our results showed that N retention in coarse roots significantly
431 contributed to whole-plant N conservation and was paralleled with a decrease in fine-root SRL,
432 SRA and N concentration, as well as an increase in RD and CR: FR ratio, suggesting a shift
433 towards longer-lived roots with lower acquisitive abilities at the end of the growing season
434 (Luke McCormack *et al.* 2012). Similarly, Wang *et al.* (2018) reported that conservative growth
435 strategies contributed to overall ecosystem ¹⁵N retention by increasing root biomass and root
436 N uptake in an alpine meadow. Because there was little difference in species abundance or
437 biomass composition in plant communities between two growing stages (Figs S1–S2), the shift
438 of nutrient strategies in plant community during senescence could be mostly explained by
439 intraspecific trait fluctuations (Figs S1–S2). These results suggest that N partitioning may be
440 temporally coordinated with plant nutrient utilization strategies, which may optimize the cost-
441 benefit of plant nutrient acquisition to match seasonal fluctuations in resource availability and
442 plant nutrient demand.

443

444 **4.3 N transfer from plants to soil organic materials during plant senescence**

445 When ^{15}N -enriched ammonium is applied to soil, some ^{15}N may enter plant biomass or
446 microbial biomass, while some may directly be absorbed into soil clay. Subsequently, ^{15}N in
447 plant roots mostly ends as POM and the more labile components of N compounds such as root
448 exudates and fine roots may be used by microbes and end up either in microbial biomass or
449 microbial necromass which mostly associate with MAOM. Therefore, there are some tradeoffs
450 between plant biomass N and SOM-N, or between POM-N and MAOM-N. But the numbers
451 are not exactly matched because some N lost from the system through gaseous emissions and
452 leaching. Since POM is largely composed of partly decomposed plant residues (Lavallee,
453 Soong & Cotrufo 2020; Cotrufo *et al.* 2022), the substantial increase in POM-N further
454 suggests that N uptake by plants and subsequent incorporation of plant-derived residues into
455 POM mainly occurred via fine-root and microbial biomass turnovers (Kuzyakov & Xu 2013;
456 Daly *et al.* 2021). Substantial ^{15}N transfer to MAOM is generally linked to soluble N forms
457 (e.g., root N leakage) and small molecular weight compounds derived from advanced
458 decomposition of plant and microbial residues or root exudates (Huysgens *et al.* 2008; De Vries
459 & Bardgett 2012; Daly *et al.* 2021; Cotrufo *et al.* 2022). The significant increases in bulk soil
460 ^{15}N , as well as POM- ^{15}N and MAOM- ^{15}N , from the peak growing season to the plant
461 senescence stage suggest the continuation of these processes during plant senescence. Direct
462 displacement of MAOM-N by injected $^{15}\text{NH}_4^+$ may have also contributed to the increased
463 MAOM- ^{15}N recovery, but our method did not allow us quantifying the proportion of this
464 displacement. Moreover, the concurrence of decreased MB ^{15}N and increased ^{15}N in MAOM
465 during plant senescence suggests that microbial mortality had contributed to ^{15}N transfer into

466 the MAOM pool (Fig. 4). In addition to changes in ^{15}N , we also observed a small, but
467 statistically significant, increase in soil pH from the peak biomass to the senescence stage
468 (Table 1). The pH increase may have occurred due to decreases in root uptake of cations, root
469 exudation of organic acids and root respirations (i.e., CO_2 release). Decreases in CO_2
470 production as a result of reduced microbial activities may also have contributed. Together, our
471 results showed that N redistribution into POM and MAOM during plant senescence constitutes
472 as an important avenue of soil N retention in the alpine meadow ecosystem.

473

474 **4.4 Conclusions and perspectives**

475 Our study with ^{15}N tracing provided direct evidence that substantial N was withdrawn from
476 senescing fine roots and aboveground tissues and the N storage was enhanced in coarse roots
477 and/or rhizomes during alpine plant senescence, thanks to an increase in both coarse root mass
478 fraction and N concentration. This work confirmed the dual role of plant roots with coarse roots
479 acting as a N storage pool and fine roots as a N depletion pool during senescence. In parallel,
480 we observed a temporal shift in plant nutrient strategies from fast acquisition during the
481 growing season to strong conservation at the non-growing season at the plant community level.
482 Overall, our findings suggest that N redistribution and seasonal plant trait fluctuation couple to
483 facilitate plant N conservation and ecosystem N retention, which may contribute to the
484 temporal coupling between plant N demand and ecosystem N supply, especially in N-limited
485 alpine ecosystems. This study clearly quantified plant shoot-root and plant-soil N redistribution
486 during senescence via a ^{15}N pool-based framework, avoiding many of the pitfalls in how N
487 resorption is typically measured, especially in roots. This work opens new perspectives for

488 mechanistic understandings of the plant nutrient economy, plant-driven C and N
489 biogeochemical cycling and their responses to environmental change, which may help improve
490 biogeochemical model predictions of plant productivity and nutrient cycling under future
491 climate change scenarios.

492

493 **Acknowledgments**

494 We thank Bin Wu, Chunlong Wang, Fuwei Wang, Chenglong Ye, Xianhui Zhou and Hui Guo
495 for their assistance in field experimental maintenance and sampling. This research was funded
496 by the National Natural Science Foundation of China (No.32171646). Qingzhou Zhao was
497 supported by the Chinese Scholarship Council (No.202206850027).

498 **Author contributions**

499 Qingzhou Zhao and Shuijin Hu conceived the idea and designed the methodology. Qingzhou
500 Zhao, Peng Wang, Lingyan Hu, Xupeng Liu collected the data. Qingzhou Zhao performed the
501 data analysis and result visualization. Qingzhou Zhao led the writing of the manuscript. Peng
502 Wang, Shuijin Hu revised the manuscript with significant inputs from all other authors. All
503 authors contributed critically to the drafts and gave final approval for publication.

504 **Competing interests**

505 The authors declare that there is no conflict of interest. Grégoire Freschet is an Associate Editor
506 of Journal of Ecology, but took no part in the peer review and decision-making processes for

507 this paper.

508 **Data availability**

509 All data needed to evaluate the conclusions in this study are present in the paper and the
510 supplementary materials. Additional data that support the findings of this study are available
511 from the corresponding author upon reasonable request.

512

513 **References**

- 514 Aerts, R. (1990) Nutrient use efficiency in evergreen and deciduous species from heathlands. *Oecologia*,
515 **84**, 391-397. <https://doi.org/https://doi.org/10.1007/BF00329765>
- 516 Aerts, R. (1996) Nutrient resorption from senescing leaves of perennials: Are there general patterns? *Journal*
517 *of Ecology*, **84**, 597-608. <https://doi.org/https://doi.org/10.2307/2261481>
- 518 Aerts, R., Bakker, C. & De Caluwe, H. (1992) Root turnover as determinant of the cycling of C, N, and P in
519 a dry heathland ecosystem. *Biogeochemistry*, **15**, 175-190.
520 <https://doi.org/https://doi.org/10.1007/BF00002935>
- 521 Aerts, R., Verhoeven, J.T.A. & Whigham, D.F. (1999) Plant-mediated controls on nutrient cycling in
522 temperate fens and bogs. *Ecology*, **80**, 2170-2181. [https://doi.org/https://doi.org/10.1890/0012-9658\(1999\)080\[2170:PMCONC\]2.0.CO;2](https://doi.org/https://doi.org/10.1890/0012-9658(1999)080[2170:PMCONC]2.0.CO;2)
- 523 Bernard, L., Basile-Doelsch, I., Derrien, D., Fanin, N., Fontaine, S., Guenet, B., Karimi, B., Marsden, C. & Maron,
524 P.A. (2022) Advancing the mechanistic understanding of the priming effect on soil organic matter
525 mineralisation. *Functional Ecology*, **36**, 1355-1377. <https://doi.org/https://doi.org/10.1111/1365-2435.14038>
- 526
527
- 528 Chapin III, F.S. & Kedrowski, R.A. (1983) Seasonal Changes in Nitrogen and Phosphorus Fractions and
529 Autumn Retranslocation in Evergreen and Deciduous Taiga Trees. *Ecology*, **64**, 376-391.
530 <https://doi.org/https://doi.org/10.2307/1937083>
- 531 Chapin III, F.S., Matson, P.A. & Vitousek, P. (2011) *Principles of terrestrial ecosystem ecology*. Springer
532 Science & Business Media.
- 533 Cong, Y., Li, M.-H., Liu, K., Dang, Y.-C., Han, H.-D. & He, H.S. (2019) Decreased Temperature with Increasing
534 Elevation Decreases the End-Season Leaf-to-Wood Reallocation of Resources in Deciduous
535 *Betula ermanii* Cham. Trees. *Forests*, **10**, 166. <https://doi.org/https://doi.org/10.3390/f10020166>
- 536 Cotrufo, M.F., Haddix, M.L., Kroeger, M.E. & Stewart, C.E. (2022) The role of plant input physical-chemical
537 properties, and microbial and soil chemical diversity on the formation of particulate and mineral-
538 associated organic matter. *Soil Biology and Biochemistry*, **168**, 108648.
539 <https://doi.org/https://doi.org/10.1016/j.soilbio.2022.108648>
- 540 Daly, A.B., Jilling, A., Bowles, T.M., Buchkowski, R.W., Frey, S.D., Kallenbach, C.M., Keiluweit, M.,
541 Mooshammer, M., Schimel, J.P. & Grandy, A.S. (2021) A holistic framework integrating plant-

542 microbe-mineral regulation of soil bioavailable nitrogen. *Biogeochemistry*, **154**, 211-229.
543 <https://doi.org/https://doi.org/10.1007/s10533-021-00793-9>

544 De Vries, F.T. & Bardgett, R.D. (2012) Plant–microbial linkages and ecosystem nitrogen retention: lessons
545 for sustainable agriculture. *Frontiers in Ecology and the Environment*, **10**, 425-432.
546 <https://doi.org/https://doi.org/10.1890/110162>

547 De Vries, F.T., Bloem, J., Quirk, H., Stevens, C.J., Bol, R. & Bardgett, R.D. (2012) Extensive management
548 promotes plant and microbial nitrogen retention in temperate grassland. *PLoS ONE*, **7**, e51201.
549 <https://doi.org/https://doi.org/10.1371/journal.pone.0051201>

550 Deng, M., Liu, L., Jiang, L., Liu, W., Wang, X., Li, S., Yang, S. & Wang, B. (2018) Ecosystem scale trade-off in
551 nitrogen acquisition pathways. *Nature Ecology & Evolution*, **2**, 1724-1734.
552 <https://doi.org/https://doi.org/10.1038/s41559-018-0677-1>

553 Du, E., Terrer, C., Pellegrini, A.F., Ahlström, A., van Lissa, C.J., Zhao, X., Xia, N., Wu, X. & Jackson, R.B. (2020)
554 Global patterns of terrestrial nitrogen and phosphorus limitation. *Nature Geoscience*, **13**, 221–226.
555 <https://doi.org/https://doi.org/10.1038/s41561-019-0530-4>

556 Eckstein, R.L., Karlsson, P. & Weih, M. (1999) Leaf life span and nutrient resorption as determinants of plant
557 nutrient conservation in temperate-arctic regions. *The New Phytologist*, **143**, 177-189.
558 <https://doi.org/https://doi.org/10.1046/j.1469-8137.1999.00429.x>

559 Fisher, J.B., Sitch, S., Malhi, Y., Fisher, R.A., Huntingford, C. & Tan, S.-Y. (2010) Carbon cost of plant nitrogen
560 acquisition: A mechanistic, globally applicable model of plant nitrogen uptake, retranslocation,
561 and fixation. *Global Biogeochemical Cycles*, **24**, GB1014.
562 <https://doi.org/https://doi.org/10.1029/2009GB003621>

563 Freschet, G.T., Cornelissen, J.H., van Logtestijn, R.S. & Aerts, R. (2010) Substantial nutrient resorption from
564 leaves, stems and roots in a subarctic flora: what is the link with other resource economics traits?
565 *New Phytologist*, **186**, 879-889. <https://doi.org/https://doi.org/10.1111/j.1469-8137.2010.03228.x>

566 Freschet, G.T., Pagès, L., Iversen, C.M., Comas, L.H., Rewald, B., Roumet, C., Klimešová, J., Zadworny, M.,
567 Poorter, H., Postma, J.A., Adams, T.S., Bagniewska-Zadworna, A., Bengough, A.G., Blancaflor, E.B.,
568 Brunner, I., Cornelissen, J.H.C., Garnier, E., Gessler, A., Hobbie, S.E., Meier, I.C., Mommer, L., Picon-
569 Cochard, C., Rose, L., Ryser, P., Scherer-Lorenzen, M., Soudzilovskaia, N.A., Stokes, A., Sun, T.,
570 Valverde-Barrantes, O.J., Weemstra, M., Weigelt, A., Wurzbürger, N., York, L.M., Batterman, S.A.,
571 Gomes De Moraes, M., Janeček, Š., Lambers, H., Salmon, V., Tharayil, N. & McCormack, M.L. (2021a)
572 A starting guide to root ecology: strengthening ecological concepts and standardising root
573 classification, sampling, processing and trait measurements. *New Phytologist*, **232**, 973-1122.
574 <https://doi.org/https://doi.org/10.1111/nph.17572>

575 Freschet, G.T., Roumet, C., Comas, L.H., Weemstra, M., Bengough, A.G., Rewald, B., Bardgett, R.D., De Deyn,
576 G.B., Johnson, D. & Klimešová, J. (2021b) Root traits as drivers of plant and ecosystem functioning:
577 current understanding, pitfalls and future research needs. *New Phytologist*, **232**, 1123-1158.
578 <https://doi.org/https://doi.org/10.1111/nph.17072>

579 Gordon, W.S. & Jackson, R.B. (2000) Nutrient concentrations in fine roots. *Ecology*, **81**, 275-280.
580 [https://doi.org/https://doi.org/10.1890/0012-9658\(2000\)081\[0275:NCIFR\]2.0.CO;2](https://doi.org/https://doi.org/10.1890/0012-9658(2000)081[0275:NCIFR]2.0.CO;2)

581 Hayes, P., Turner, B.L., Lambers, H., Laliberté, E. & Bellingham, P. (2014) Foliar nutrient concentrations and
582 resorption efficiency in plants of contrasting nutrient-acquisition strategies along a 2-million-year
583 dune chronosequence. *Journal of Ecology*, **102**, 396-410.
584 <https://doi.org/https://doi.org/10.1111/1365-2745.12196>

585 Hu, S., Chapin, F.S., Firestone, M.K., Field, C.B. & Chiariello, N.R. (2001) Nitrogen limitation of microbial

586 decomposition in a grassland under elevated CO₂. *Nature*, **409**, 188-191.
587 <https://doi.org/https://doi.org/10.1038/35051576>

588 Huygens, D., Boeckx, P., Templer, P., Paulino, L., Van Cleemput, O., Oyarzún, C., Müller, C. & Godoy, R.
589 (2008) Mechanisms for retention of bioavailable nitrogen in volcanic rainforest soils. *Nature*
590 *Geoscience*, **1**, 543-548. <https://doi.org/https://doi.org/10.1038/ngeo252>

591 Jia, Z., Li, P., Wu, Y., Chang, P., Deng, M., Liang, L., Yang, S., Wang, C., Wang, B., Yang, L., Wang, X., Wang,
592 Z., Peng, Z., Guo, L., Ahirwal, J., Liu, W. & Liu, L. (2022) Deepened snow loosens temporal coupling
593 between plant and microbial N utilization and induces ecosystem N losses. *Global Change Biology*,
594 **28**, 4655– 4667. <https://doi.org/https://doi.org/10.1111/gcb.16234>

595 Jilling, A., Keiluweit, M., Contosta, A.R., Frey, S., Schimel, J., Schneck, J., Smith, R.G., Tiemann, L. & Grandy,
596 A.S. (2018) Minerals in the rhizosphere: overlooked mediators of soil nitrogen availability to plants
597 and microbes. *Biogeochemistry*, **139**, 103-122. [https://doi.org/https://doi.org/10.1007/s10533-](https://doi.org/https://doi.org/10.1007/s10533-018-0459-5)
598 [018-0459-5](https://doi.org/https://doi.org/10.1007/s10533-018-0459-5)

599 Joswig, J.S., Wirth, C., Schuman, M.C., Kattge, J., Reu, B., Wright, I.J., Sippel, S.D., Rüger, N., Richter, R.,
600 Schaeppman, M.E., Van Bodegom, P.M., Cornelissen, J.H.C., Díaz, S., Hattingh, W.N., Kramer, K., Lens,
601 F., Niinemets, Ü., Reich, P.B., Reichstein, M., Römermann, C., Schrodt, F., Anand, M., Bahn, M., Byun,
602 C., Campetella, G., Cerabolini, B.E.L., Craine, J.M., Gonzalez-Melo, A., Gutiérrez, A.G., He, T., Higuchi,
603 P., Jactel, H., Kraft, N.J.B., Minden, V., Onipchenko, V., Peñuelas, J., Pillar, V.D., Sosinski, Ê.,
604 Soudzilovskaia, N.A., Weiher, E. & Mahecha, M.D. (2021) Climatic and soil factors explain the two-
605 dimensional spectrum of global plant trait variation. *Nature Ecology & Evolution*, **6**, 36–50.
606 <https://doi.org/https://doi.org/10.1038/s41559-021-01616-8>

607 Keep, T., Sampoux, J.P., Barre, P., Blanco-Pastor, J.L., Dehmer, K.J., Durand, J.L., Hegarty, M., Ledauphin, T.,
608 Muylle, H., Roldán-Ruiz, I., Ruttink, T., Surault, F., Willner, E. & Volaire, F. (2021) To grow or survive:
609 Which are the strategies of a perennial grass to face severe seasonal stress? *Functional Ecology*,
610 **35**, 1145-1158. <https://doi.org/https://doi.org/10.1111/1365-2435.13770>

611 Kunkle, J.M., Walters, M.B. & Kobe, R.K. (2009) Senescence-related changes in nitrogen in fine roots: mass
612 loss affects estimation. *Tree Physiology*, **29**, 715-723.
613 <https://doi.org/https://doi.org/10.1093/treephys/tpp004>

614 Kuzyakov, Y. & Xu, X. (2013) Competition between roots and microorganisms for nitrogen: mechanisms
615 and ecological relevance. *New Phytologist*, **198**, 656-669.
616 <https://doi.org/https://doi.org/10.1111/nph.12235>

617 Lambers, H., Chapin III, F.S. & Pons, T.L. (2008) *Plant physiological ecology*, 2 edn. Springer Science &
618 Business Media.

619 Lambers, H., Raven, J.A., Shaver, G.R. & Smith, S.E. (2008) Plant nutrient-acquisition strategies change with
620 soil age. *Trends in Ecology & Evolution*, **23**, 95-103.
621 <https://doi.org/https://doi.org/10.1016/j.tree.2007.10.008>

622 Lavallee, J.M., Soong, J.L. & Cotrufo, M.F. (2020) Conceptualizing soil organic matter into particulate and
623 mineral-associated forms to address global change in the 21st century. *Global Change Biology*,
624 **26**, 261-273. <https://doi.org/https://doi.org/10.1111/gcb.14859>

625 Lü, X.-T., Hou, S.-L., Reed, S., Yin, J.-X., Hu, Y.-Y., Wei, H.-W., Zhang, Z.-W., Yang, G.-J., Liu, Z.-Y. & Han,
626 X.-G. (2021) Nitrogen Enrichment Reduces Nitrogen and Phosphorus Resorption Through
627 Changes to Species Resorption and Plant Community Composition. *Ecosystems*, **24**, 602-612.
628 <https://doi.org/https://doi.org/10.1007/s10021-020-00537-0>

629 Lü, X.T., Hu, Y.Y., Wolf, A.A., Han, X.G. & Le Bagousse-Pinguet, Y. (2019) Species richness mediates within-

630 species nutrient resorption: Implications for the biodiversity–productivity relationship. *Journal of*
631 *Ecology*, **107**, 2346–2352. <https://doi.org/https://doi.org/10.1111/1365-2745.13180>

632 Luke McCormack, M., Adams, T.S., Smithwick, E.A.H. & Eissenstat, D.M. (2012) Predicting fine root lifespan
633 from plant functional traits in temperate trees. *New Phytologist*, **195**, 823–831.
634 <https://doi.org/https://doi.org/10.1111/j.1469-8137.2012.04198.x>

635 Ma, H., Mo, L., Crowther, T.W., Maynard, D.S., Van Den Hoogen, J., Stocker, B.D., Terrer, C. & Zohner, C.M.
636 (2021) The global distribution and environmental drivers of aboveground versus belowground
637 plant biomass. *Nature Ecology & Evolution*, **5**, 1110–1122.
638 <https://doi.org/https://doi.org/10.1038/s41559-021-01485-1>

639 McCormack, M.L., Dickie, I.A., Eissenstat, D.M., Fahey, T.J., Fernandez, C.W., Guo, D., Helmisaari, H.S., Hobbie,
640 E.A., Iversen, C.M. & Jackson, R.B. (2015) Redefining fine roots improves understanding of below-
641 ground contributions to terrestrial biosphere processes. *New Phytologist*, **207**, 505–518.
642 <https://doi.org/https://doi.org/10.1111/nph.13363>

643 Meier, C.E., Grier, C.C. & Cole, D.W. (1985) Below- and aboveground N and P use by *Abies amabilis* stands.
644 *Ecology*, **66**, 1928–1942. <https://doi.org/https://doi.org/10.2307/2937389>

645 Millard, P. & Grelet, G.-a. (2010) Nitrogen storage and remobilization by trees: ecophysiological relevance
646 in a changing world. *Tree Physiology*, **30**, 1083–1095.
647 <https://doi.org/https://doi.org/10.1093/treephys/tpq042>

648 Nambiar, E.S. (1987) Do nutrients retranslocate from fine roots? *Canadian Journal of Forest Research*, **17**,
649 913–918. <https://doi.org/https://doi.org/10.1139/x87-143>

650 Ni, J. (2000) A simulation of biomes on the Tibetan Plateau and their responses to global climate change.
651 *Mountain Research and Development*, **20**, 80–89. [https://doi.org/https://doi.org/10.1659/0276-4741\(2000\)020\[0080:ASOBOT\]2.0.CO;2](https://doi.org/https://doi.org/10.1659/0276-4741(2000)020[0080:ASOBOT]2.0.CO;2)

652 Parton, W., Silver, W.L., Burke, I.C., Grassens, L., Harmon, M.E., Currie, W.S., King, J.Y., Adair, E.C., Brandt,
653 L.A., Hart, S.C. & Fasth, B. (2007) Global-scale similarities in nitrogen release patterns during long-
654 term decomposition. *Science*, **315**, 361–364.
655 <https://doi.org/https://doi.org/10.1126/science.1134853>

656 R, C.t. (2021) R: A language and environment for statistical computing. *R Foundation for Statistical*
657 *Computing, Vienna*. <https://doi.org/https://www.R-project.org>

658 Reich, P.B. (2014) The world-wide ‘fast-slow’ plant economics spectrum: a traits manifesto. *Journal of*
659 *Ecology*, **102**, 275–301. <https://doi.org/https://doi.org/10.1111/1365-2745.12211>

660 Schimel, J.P. & Bennett, J. (2004) Nitrogen mineralization: challenges of a changing paradigm. *Ecology*, **85**,
661 591–602. <https://doi.org/https://doi.org/10.1890/03-8002>

662 Shahzad, T., Chenu, C., Repinçay, C., Mougin, C., Ollier, J.-L. & Fontaine, S. (2012) Plant clipping decelerates
663 the mineralization of recalcitrant soil organic matter under multiple grassland species. *Soil Biology*
664 *and Biochemistry*, **51**, 73–80. <https://doi.org/https://doi.org/10.1016/j.soilbio.2012.04.014>

665 Sollins, P., Homann, P. & Caldwell, B.A. (1996) Stabilization and destabilization of soil organic matter:
666 mechanisms and controls. *Geoderma*, **74**, 65–105. [https://doi.org/https://doi.org/10.1016/S0016-7061\(96\)00036-5](https://doi.org/https://doi.org/10.1016/S0016-7061(96)00036-5)

667 Stark, J.M. & Hart, S.C. (1996) Diffusion technique for preparing salt solutions, Kjeldahl digests, and
668 persulfate digests for nitrogen-15 analysis. *Soil Science Society of America Journal*, **60**, 1846–1855.
669 <https://doi.org/https://doi.org/10.2136/sssaj1996.03615995006000060033x>

670 van Heerwaarden, L.M., Toet, S. & Aerts, R. (2003) Current measures of nutrient resorption efficiency lead
671 to a substantial underestimation of real resorption efficiency: facts and solutions. *Oikos*, **101**, 664–
672

674 669. <https://doi.org/https://doi.org/10.1034/j.1600-0706.2003.12351.x>

675 Vergutz, L., Manzoni, S., Porporato, A., Novais, R.F. & Jackson, R.B. (2012) Global resorption efficiencies and
676 concentrations of carbon and nutrients in leaves of terrestrial plants. *Ecological Monographs*, **82**,
677 205-220. <https://doi.org/https://doi.org/10.1890/11-0416.1>

678 Vitra, A., Deléglise, C., Meisser, M., Risch, A.C., Signarbieux, C., Lamacque, L., Delzon, S., Buttler, A. &
679 Mariotte, P. (2019) Responses of plant leaf economic and hydraulic traits mediate the effects of
680 early- and late-season drought on grassland productivity. *AoB PLANTS*, **11**, plz023.
681 <https://doi.org/https://doi.org/10.1093/aobpla/plz023>

682 Wang, F., Shi, G., Nicholas, O., Yao, B., Ji, M., Wang, W., Ma, Z., Zhou, H. & Zhao, X. (2018) Ecosystem
683 nitrogen retention is regulated by plant community trait interactions with nutrient status in an
684 alpine meadow. *Journal of Ecology*, **106**, 1570-1581.
685 <https://doi.org/https://doi.org/10.1111/1365-2745.12924>

686 Wang, P., Guo, J., Xu, X., Yan, X., Zhang, K., Qiu, Y., Zhao, Q., Huang, K., Luo, X., Yang, F., Guo, H. & Hu, S.
687 (2020) Soil acidification alters root morphology, increases root biomass but reduces root
688 decomposition in an alpine grassland. *Environmental pollution*, **265**, 115016.
689 <https://doi.org/https://doi.org/10.1016/j.envpol.2020.115016>

690 Weigelt, A., Mommer, L., Andraczek, K., Iversen, C.M., Bergmann, J., Bruelheide, H., Fan, Y., Freschet, G.T.,
691 Guerrero-Ramírez, N.R., Kattge, J., Kuyper, T.W., Laughlin, D.C., Meier, I.C., Plas, F., Poorter, H.,
692 Roumet, C., Ruijven, J., Sabatini, F.M., Semchenko, M., Sweeney, C.J., Valverde-Barrantes, O.J., York,
693 L.M. & McCormack, M.L. (2021) An integrated framework of plant form and function: the
694 belowground perspective. *New Phytologist*, **232**, 42-59.
695 <https://doi.org/https://doi.org/10.1111/nph.17590>

696 Woodmansee, R., Vallis, I. & Mott, J. (1981) Grassland nitrogen. *Ecological Bulletins*, **33**, 443-462.
697 <https://doi.org/https://www.jstor.org/stable/45128681>

698 Xu, X., Qiu, Y., Zhang, K., Yang, F., Chen, M., Luo, X., Yan, X., Wang, P., Zhang, Y. & Chen, H. (2021) Climate
699 warming promotes deterministic assembly of arbuscular mycorrhizal fungal communities. *Global
700 Change Biology*, **28**, 1147-1161. <https://doi.org/https://doi.org/10.1111/gcb.15945>

701 Yan, D., Wang, D. & Yang, L. (2007) Long-term effect of chemical fertilizer, straw, and manure on labile
702 organic matter fractions in a paddy soil. *Biology and Fertility of Soils*, **44**, 93-101.
703 <https://doi.org/https://doi.org/10.1007/s00374-007-0183-0>

704 Yang, Y., Fang, J., Ji, C. & Han, W. (2009) Above- and belowground biomass allocation in Tibetan grasslands.
705 *Journal of Vegetation Science*, **20**, 177-184. [https://doi.org/https://doi.org/10.1111/j.1654-
706 1103.2009.05566.x](https://doi.org/https://doi.org/10.1111/j.1654-1103.2009.05566.x)

707 Yuan, Z.Y. & Chen, H.Y.H. (2009) Global-scale patterns of nutrient resorption associated with latitude,
708 temperature and precipitation. *Global Ecology and Biogeography*, **18**, 11-18.
709 <https://doi.org/https://doi.org/10.1111/j.1466-8238.2009.00474.x>

710 Zadworny, M., McCormack, M.L., Rawlik, K. & Jagodziński, A.M. (2015) Seasonal variation in chemistry, but
711 not morphology, in roots of *Quercus robur* growing in different soil types. *Tree Physiology*, **35**,
712 644-652. <https://doi.org/https://doi.org/10.1093/treephys/tpv018>

713 Zhang, Y., Zhang, N., Yin, J., Zhao, Y., Yang, F., Jiang, Z., Tao, J., Yan, X., Qiu, Y., Guo, H. & Hu, S. (2020)
714 Simulated warming enhances the responses of microbial N transformations to reactive N input in
715 a Tibetan alpine meadow. *Environment International*, **141**, 105795.
716 <https://doi.org/https://doi.org/10.1016/j.envint.2020.105795>

717 Zhao, Q., Guo, J., Shu, M., Wang, P. & Hu, S. (2020) Impacts of drought and nitrogen enrichment on leaf

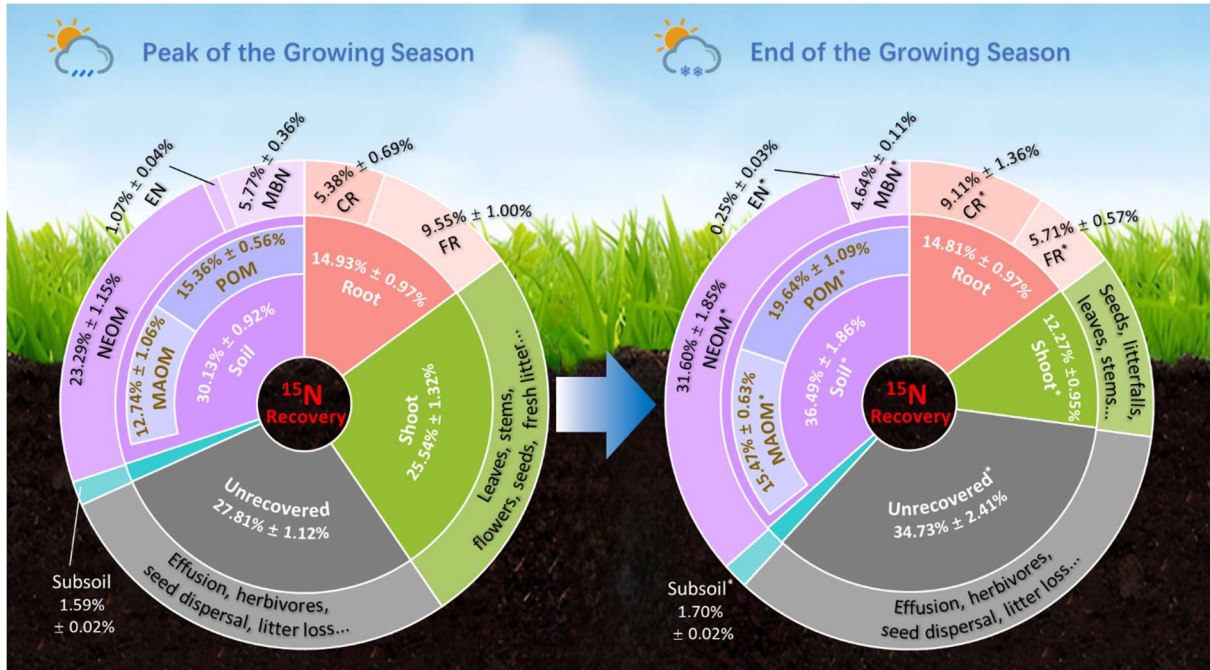
718 nutrient resorption and root nutrient allocation in four Tibetan plant species. *Science of the Total*
719 *Environment*, **723**, 138106. [https://doi.org/https://doi.org/10.1016/j.scitotenv.2020.138106](https://doi.org/10.1016/j.scitotenv.2020.138106)
720

721 Table 1. Soil and microbial properties of the topsoil (0 - 20 cm) in the ¹⁵N labeled mesocosms
 722 at different growing stages. Values are mean ± standard error (n = 6). Bold values indicate
 723 significant differences between growing stages (*P* < 0.05).

Soil & microbial properties	Peak growth of vegetation	End of the growing season	<i>P</i> -value (Paired t-test)
Soil moisture (%)	51.90% ± 1.11%	51.68% ± 1.83%	0.907
pH (H ₂ O)	5.71 ± 0.03	5.85 ± 0.04	0.032
NH ₃ ⁺ (mg kg ⁻¹)	1.25 ± 0.17	1.44 ± 0.18	0.560
NO ₃ ⁻ (mg kg ⁻¹)	24.26 ± 2.15	12.74 ± 1.37	0.005
AP (mg kg ⁻¹)	4.99 ± 0.14	4.10 ± 0.09	0.002
DOC (mg kg ⁻¹)	304.83 ± 21.90	195.73 ± 11.45	0.007
DON (mg kg ⁻¹)	79.12 ± 2.48	37.14 ± 2.34	< 0.001
MBC (mg kg ⁻¹)	1240.30 ± 65.13	731.32 ± 55.26	0.004
MBN (mg kg ⁻¹)	231.93 ± 9.56	163.70 ± 3.55	< 0.001
MBC/MBN	5.34 ± 0.12	4.48 ± 0.34	0.054
POM-C (g kg ⁻¹)	21.45 ± 1.57	18.62 ± 1.63	0.106
POM-N (g kg ⁻¹)	1.56 ± 0.14	1.30 ± 0.13	0.099
POM-C/N	13.91 ± 0.32	14.37 ± 0.22	0.185
MAOM-C (g kg ⁻¹)	34.87 ± 1.48	36.08 ± 1.16	0.469
MAOM-N (g kg ⁻¹)	3.04 ± 0.13	3.18 ± 0.09	0.343
MAOM-C/N	11.48 ± 0.08	11.33 ± 0.08	0.147

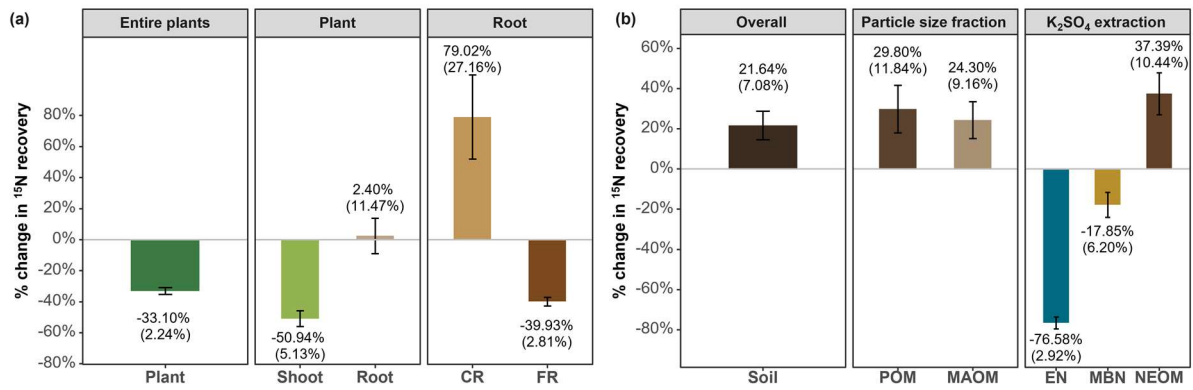
724
 725 Abbreviations: AP, soil available phosphorus; DOC, dissolved organic C; DON, dissolved
 726 organic N; MBC, soil microbial biomass C; MBN, microbial biomass N; POM, particulate
 727 organic matter (particle size > 53 μm); MAOM, mineral-associated organic matter (particle
 728 size ≤ 53 μm).

729



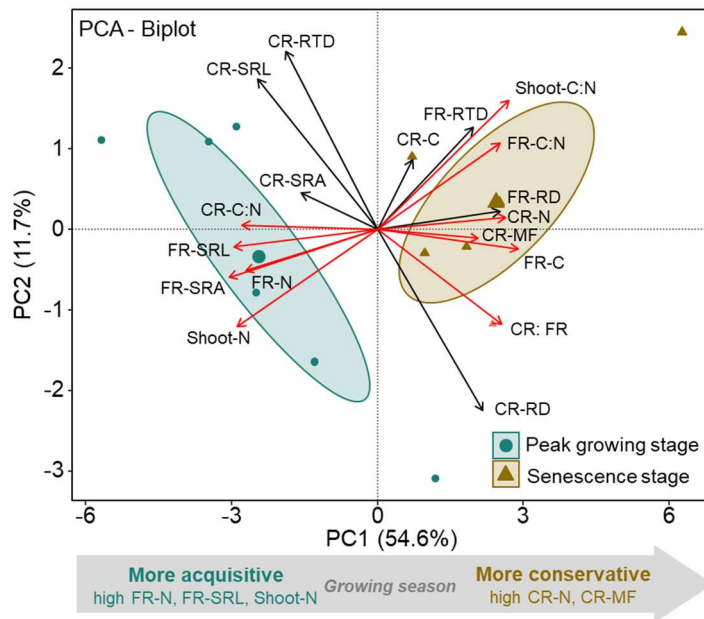
730

731 Fig. 1. ^{15}N partitioning among plant shoots, roots, soil, and their sub-fractions, a. at the peak of
 732 vegetation growth, and b. at the end of the growing season. Total microbial biomass ^{15}N in soil
 733 was calculated from microbial biomass ^{15}N flush using an extraction efficiency of 0.45. Values
 734 are mean \pm standard error ($n = 6$). The asterisk, * in b, indicates a significant difference between
 735 growing stages ($P < 0.05$). Abbreviations: NEOM, non-extractable soil organic matter; EN,
 736 K_2SO_4 extractable N; MBN, microbial biomass N; CR, coarse root (transportive roots and
 737 rhizomes, root order ≥ 3); FR, fine roots (absorptive roots, root order < 3); POM, particulate
 738 organic matter (particle size $> 53 \mu\text{m}$); MAOM, mineral-associated organic matter (particle
 739 size $\leq 53 \mu\text{m}$).



740

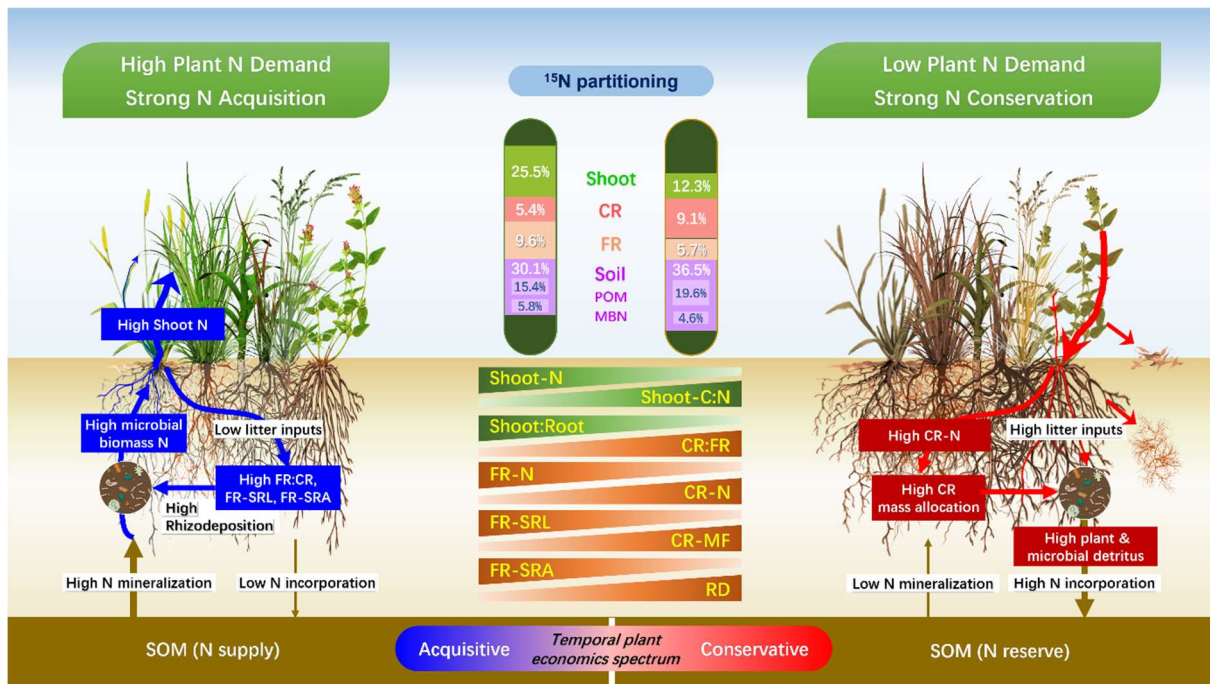
741 Fig. 2. The percentage change in ¹⁵N recovery in plant-soil N pools. (a), In whole plants, shoots,
 742 roots, coarse roots, and fine roots, and (b), in soil and soil sub-fractions during plant senescence
 743 from peak growth stage to the end of the growing season. Positive values indicate ¹⁵N storage
 744 pools and negative values indicate ¹⁵N depletion pools during plant senescence. Plants were
 745 separated into shoots and roots (all above- and below-ground biomass, respectively), and roots
 746 were further classified between coarse organs (CR, transport roots and rhizomes, root order \geq
 747 3) and fine roots (FR, absorptive roots, root order $<$ 3). The soil was divided into several
 748 fractions, depending on particle size and K₂SO₄ extractability. Values are mean (\pm standard
 749 error) (n = 6). Abbreviations: POM, particulate organic matter (particle size $>$ 53 μ m); MAOM,
 750 mineral-associated organic matter (particle size \leq 53 μ m); EN, K₂SO₄ extractable N; MBN,
 751 microbial biomass N; NEOM, non-extractable soil organic matter.



752

753 Fig. 3. Results of principal component analysis (PCA) coded by different growth stages for
 754 plant economics spectrum, including 16 root traits and two shoot traits with 95% prediction
 755 ellipses. Red arrows represent significantly-changed traits during senescence ($P < 0.05$).
 756 Belowground traits are differentiated between those of coarse belowground organs (CR,
 757 transport roots and rhizomes, root order ≥ 3) and fine roots (FR, absorptive roots, root order
 758 < 3). Abbreviations: RD, root diameter; SRL, specific root length; SRA, specific root area;
 759 RTD, root tissue density; C, carbon concentration; N, nitrogen concentration; C:N, ratio of C
 760 to N concentrations; CR:FR, ratio of CR to FR biomass.

761



762

763

764 Fig. 4. Conceptual summary of temporal plant-soil N dynamics during plant senescence, and

765 shift in plant economics traits, as a potential mechanism for minimizing N losses and improving

766 the coupling between plant N demand and bioavailable N supply in a N-limiting alpine

767 ecosystem. Abbreviations: Shoot:Root represents here the biomass ratio of all above- to below-

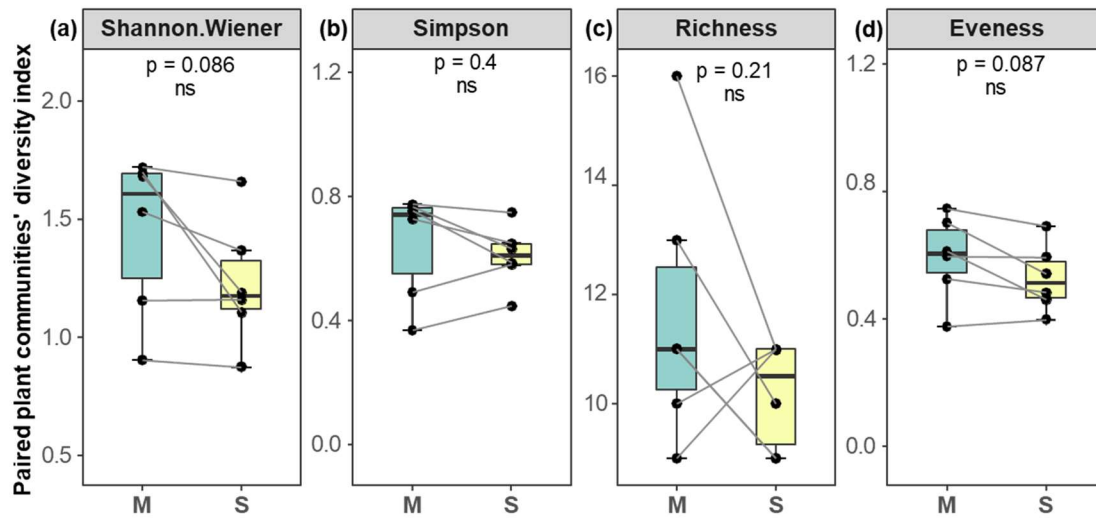
768 ground organs; CR, coarse roots (transportive roots, root order ≥ 3) and rhizomes; FR, fine

769 roots (absorptive roots, root order < 3); POM, particulate organic matter (particle size $> 53 \mu\text{m}$);

770 MBN, microbial biomass N; N, nitrogen concentration; RD, root diameter; SRL, specific root

771 length; SRA, specific root area.

772



773

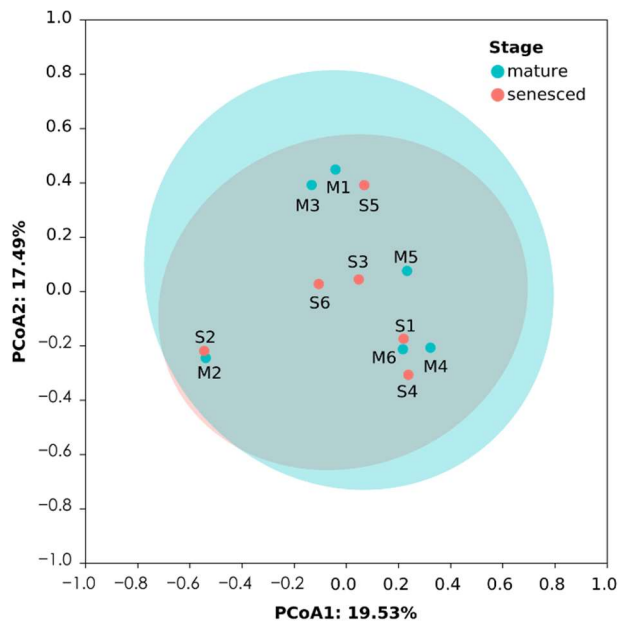
774 Figure S1. Paired plant communities' diversity indices between different growing stages. M,

775 mature stage at the peak of vegetation growth; S, senescence stage at the end of the growing

776 season. Black dots and lines are paired observations. The *P*-values and significance levels of

777 student's paired t-tests are displayed.

778



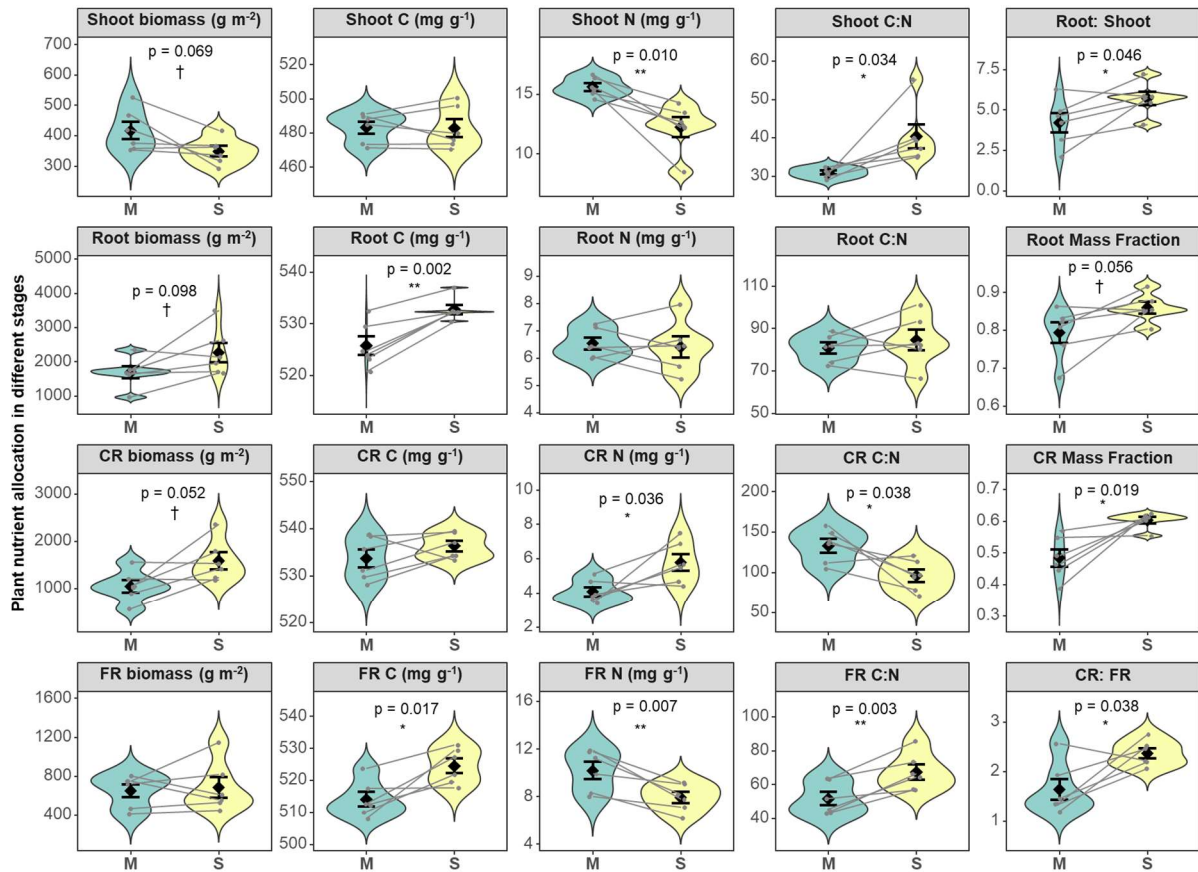
779

780 Figure S2. Principal coordinates analysis (PCoA) of the overall differences between species

781 aboveground biomass of the plant communities at two growing stages based on Bray-Curtis

782 distances under Robust Scaler standardization.

783



784

785 Fig. S3. Above- and below-ground plant nutrient allocation in different growing stages.

786 Abbreviations: M, mature stage at the peak of vegetation growth; S, senescence stage at the

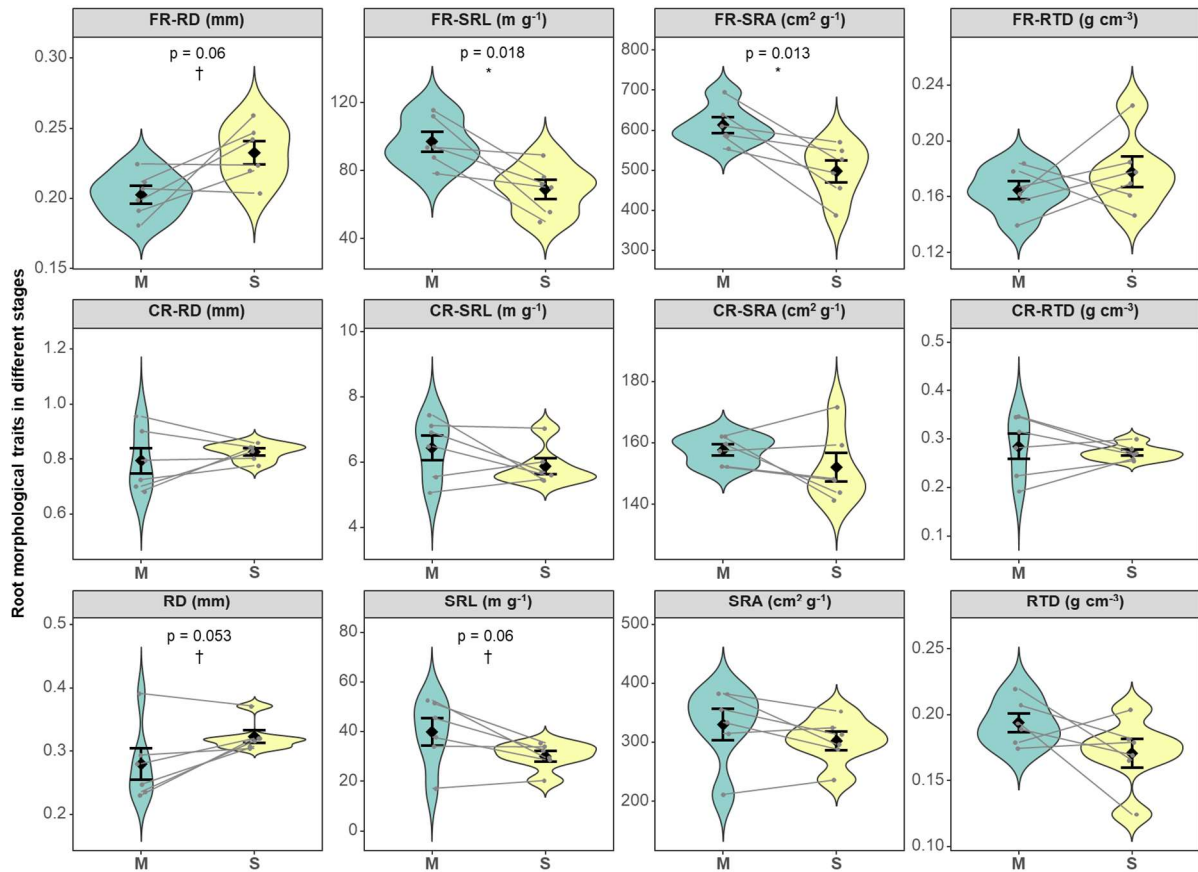
787 end of the growing season. CR, coarse roots (transportive roots, root order ≥ 3) and rhizomes;

788 FR, fine roots (absorptive roots, root order < 3); C: N, ratio of C to N concentration; Root:

789 Shoot, biomass ratio of all below- to above-ground organs. Grey dots and lines are paired

790 observations. Mean \pm SE ($n = 6$) is shown as black point and dumbbell. The P -values and

791 significance levels are labeled with † $0.05 < P < 0.10$; * $0.01 < P \leq 0.05$; ** $0.001 < P \leq 0.01$.



792

793 Fig. S4. Morphological traits of fine roots (FR), coarse belowground organs (CR: transport

794 roots and rhizomes) and all belowground organs at different growing stages. Abbreviations: M,

795 mature stage at the peak of vegetation growth; S, senescence stage at the end of the growing

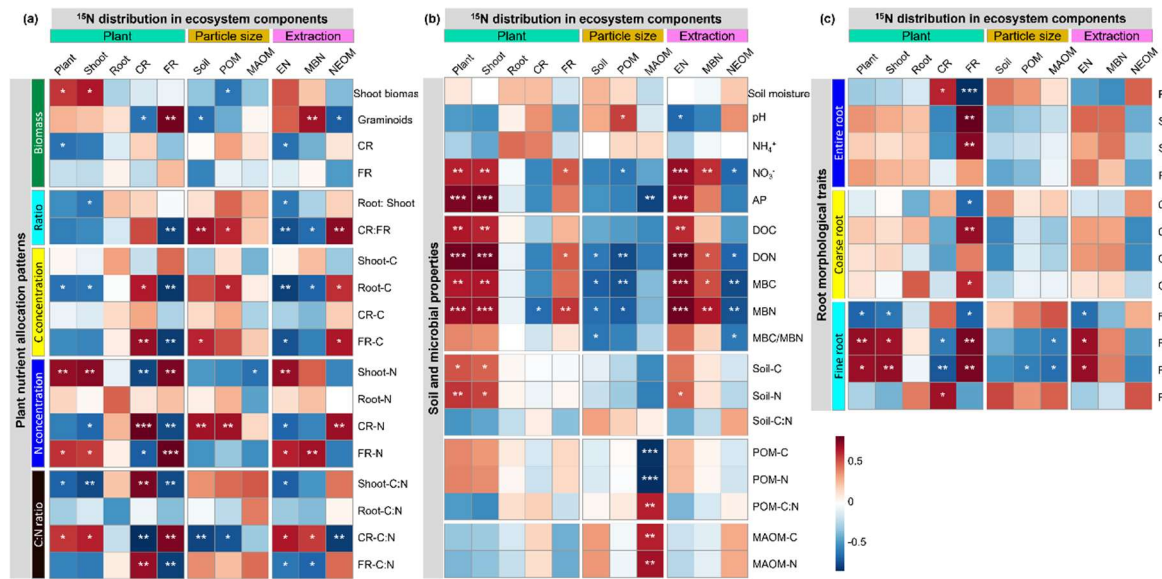
796 season. RD, root diameter; SRL, specific root length; SRA, specific root area; RTD, root tissue

797 density. Grey dots and lines are paired observations. Mean \pm standard error ($n = 6$) is shown as

798 black point and dumbbell. The P-values and significance levels are labeled with † $0.05 < P <$

799 0.10 ; * $0.01 < P \leq 0.05$.

800



801

802 Fig. S5. Pearson correlation coefficients between ^{15}N recovery rate and plant nutrient allocation

803 (a), soil and microbial properties (b), and root morphological traits (c) across the growing

804 season. Red indicates positive correlations, and blue indicates negative correlations. Darker

805 colors are associated with stronger correlation coefficients. The significance levels are labeled

806 with * $0.01 < P \leq 0.05$; ** $0.001 < P \leq 0.01$; *** $P \leq 0.001$. Abbreviations: Root, all

807 belowground organs; CR, coarse roots (transportive roots, root order ≥ 3) and rhizomes; FR,

808 fine roots (absorptive roots, root order < 3); Root:Shoot, biomass ratio of all below- to above-

809 ground organs; POM, particulate organic matter (particle size $> 53 \mu\text{m}$); MAOM, mineral-

810 associated organic matter (particle size $\leq 53 \mu\text{m}$); EN, K_2SO_4 extractable N; MBC, microbial

811 biomass C; MBN, microbial biomass N; NEOM, non-extractable soil organic matter; C, carbon

812 concentration; N, nitrogen concentration; NH_4^+ , soil ammonium concentration; NO_3^- , soil

813 nitrate concentration; AP, available soil phosphorus; DOC, dissolved organic C; DON,

814 dissolved organic N; RD, root diameter; SRL, specific root length; SRA, specific root area;

815 RTD, root tissue density.

816